

Report for the Degree of Licentiate of Engineering

Condensation of Zeotropic Refrigerant Mixtures in Shell-and-Tube Condensers

by

Dave Sajjan



Department of Heat and Power Technology
Chalmers University of Technology
S-412 58 Göteborg, Sweden

Göteborg 1999

Licentiate report

School of Chemical Engineering
Postgraduate Programme: Chemical Engineering
Department of Heat and Power Technology
Chalmers University of Technology

ISSN 1130-2952
ISRN CTH-VOM-PB--3/99-SE

Printed by Chalmers Reproservice
Göteborg 1999

Abstract

Today, HCFC-22 or R22 is an extremely safe, proven and effective refrigerant, widely used in HVAC&R industry. Since it contains chlorine suspected of ozone depletion, it needs to be replaced by a more environmentally friendly refrigerant. Some mixtures of refrigerants are believed to be ideal matches to offer about the same capacities and performance as HCFC-22, without any painstaking equipment changes. However, replacement of R22 with R407C, a zeotropic mixture, has shown that the condenser performance may fall severely, by up to 70%, compared to R22 at lower effect or at low temperature differences between the gas and the coolant media. As such experiences might reduce the willingness to convert from R22, the causes of this kind of performance deterioration need to be understood. In the present work an approach is made to identifying the main differences in condensation processes of a pure fluid and a mixture.

Since the local thermodynamic parameters (condensing temperature, latent heat etc.) and transport rates are directly related to local vapour and condensate compositions, the paths of the liquid and gas in the condenser influence the performance. Most calculation methods assume the most favourable conditions, i.e. that the gas and condensate streams are well mixed and that they accompany each other through the condenser. In this work, the effects of deviation from these conditions are studied for shell-side condensation.

A detailed computer simulation program is developed, taking into account both mass transfer resistance in the gas phase and the mixing in the condensate layer, where a parameter that varies between two extreme cases of the condensation curve, the integral where the condensate and the gas vapour are in intimate contact and the differential representing the segregation of the gas vapour, is introduced. Setting this parameter to an intermediate value made the calculated results coincide with those found experimentally. It was also found, for one of the conditions studied, that

- a decrease in condensation rate of the order of 8% is observed due to mass transfer resistance;
- at lower mass flux and at lower temperature differences between the gas and the coolant, the resistance to heat transfer lies in the vapour film and the condensation curve is more close to differential.

Some connections between the gas flow-pattern and the condensation rates have been analyzed using a CFD program. An enhancement in condensation rates of the order of 15% was observed by decreasing the shell-side by-pass and making design changes at the gas inlet.

Keywords—multicomponent, condensation, shell-and-tube condenser, zeotropic refrigerant mixture, R407C, mass transfer resistance, condensate mixing.

List of Contents

Abstract	iii
List of Contents	v
Table of Nomenclature	viii
1. Introduction	1
1.1 Introduction to air conditioning	1
1.2 Vapour compression chiller	1
1.3 Condenser	1
1.4 Shell and tube condenser	2
1.5 Working fluids	2
1.6 Consequences of zeotropic mixtures in condensers (literature review)	3
1.7 Aim of this thesis	4
1.8 Program Climate 21	5
1.9 Organization of the thesis	5
2. Important concepts	7
2.1 Condensation of zeotropic mixtures	7
2.1.1 Silver's Method	8
2.1.2 Multicomponent condensation based on film theory	8
2.1.3 Gas-phase mass transport	9
2.2 Energy balances and heat transfer rate relations	10
2.3 Condensation curves	11
2.4 Heat transfer coefficient in condensate layer	14
2.5 Effect of inundation	16
2.5.1 Effect of surface tension on film condensation	16
2.5.2 Effect of vapour shear	17
2.6 Heat transfer coefficient and enhancement ratio	17

3. CFD and the condenser design	19
3.1 Introduction	19
3.2 What is CFD modelling?	20
3.2.1 Choice of the CFD program	20
3.3 Simplifying assumptions	21
4. Results and summary of papers	23
4.1 Paper I: “Reasons for drop in shell-and-tube condenser performance when replacing R22 with R407C”	23
4.1.1 Comparison of condenser performance	23
4.1.2 Performance comparison of pure (R22) and mixed working fluid (R407C)	24
4.2 Paper II: “Influence of condenser design on flow pattern and performance of shell-and-tube condenser for zeotropic refrigerant mixture”	24
5. Conclusions and recommendations	27
5.1 Conclusions	27
5.2 Recommendations	28
6. Acknowledgements	29
7. References	31

This report is based on work reported in the following papers, referred to by Roman numerals in the text:

- I. D. Sajjan, L. Vamling: “Reasons for drop in shell-and-tube condenser performance when replacing R22 with R407C”.
- II. D. Sajjan, L. Vamling: “Influence of condenser design on flow pattern and performance of shell-and-tube condenser for zeotropic refrigerant mixture”.

Table of Nomenclature

A_o	outside surface area of tube (m^2/m)
A_f	surface area of fins (m^2/m)
A_r	surface area of tube with fin-root diameter (m^2/m)
A_t	inside surface area of tube (m^2/m)
C	molar density (mol/m^3)
C_p	heat capacity ($J/mol\ k$)
d_{eq}	equivalent diameter (m)
d_f	diameter to the outside of fin tips (m)
d_r	diameter to the fin roots (m)
D_{ij}	diffusion coefficient of component “i” in “j”
g	gravitational acceleration (m/s^2)
G	gas flow (kg/ m^2s)
H_f	fin height (m)
h_{fg}	specific enthalpy of vapourization (J/kg)
h_g	heat transfer coefficient for the gas film (W/ m^2K)
h_c	heat transfer coefficient on the coolant side (W/ m^2K)
h_l	heat transfer coefficient for the condensate (W/ m^2K)
h_L	heat transfer coefficient from interface to the coolant (W/ m^2K)
h_m	gas-liquid mixture enthalpy (J/mol)
j	heat and mass transfer factor (equation 4)
k	thermal conductivity (W/mK)
M_m	mean molar weight of the mixture (kg/mol)
M_c	molar weight of the coolant (kg/mol)
m_c	coolant mass flow rate (kg/s)
N	tube number in tube-bank
N_i	molar flux of component “i” towards the interface (mol/ m^2s)
N_{tot}	total molar flux (mol/ m^2s)
p	total pressure (Pa)
q_L	heat flux from the interface to the coolant (W/m^2)
q_g	heat flux from the gas bulk to the interface (W/m^2)
R	molar gas constant ($J/mol\ K$)
R_t, R_s	fouling resistance on tube and shell side (m^2K/W)
T_c	coolant temperature (K)
T_b	bulk gas temperature (K)
T_I	interface temperature (K)
U	overall heat transfer coefficient with respect to total outer surface area (W/ m^2K)
\mathbf{x}_I	vector of molar fractions of components in condensate at the interface
y_b	mole fraction of component “b” in the gas bulk
\mathbf{y}_I	vector of gas phase molar fractions of components at the interface
z	co-ordinate (m)

λ_w	wall thermal conductivity (W/mK)
gas	film thickness (m)
δ_w	tube wall thickness (m)
κ_{ij}	mass transfer coefficient (mol/ m ² s)
μ	dynamic viscosity (kg/ms)
ρ	density (kg/m ³)

Superscripts and subscripts

C	coolant
g	gas phase
i	component ‘i’ in the mixture
l	condensate
int	Integral (when condensate is assumed to be completely mixed)
diff	Differential (no condensate mixing takes place)

1. Introduction

1.1 Introduction to air conditioning

Air conditioning and refrigeration are more than just a luxury in today's world. Much of the way we live is determined by air conditioning. The system by which modern air conditioners function is called the vapour-compression refrigeration cycle. The function of this system is to pick up heat at one location (inside) and to dispose of it in another location (outside).

1.2 Vapour compression chiller

A chiller, which is at the heart of large air-conditioning systems, is a machine built to satisfy a need for cooling via the chilling of a fluid, most commonly water. Chillers can be categorized as one of two basic types: those that employ a mechanical vapour compression cycle with a refrigerant, and those that use a chemical absorption process with water as the refrigerant.

There are four basic components in a mechanical vapour-compression refrigeration cycle: a compressor, a condenser, an evaporator, and an expansion device. The system works by pumping a substance, known as the refrigerant or working fluid, through these components, while it warms and cools. The heat exchangers (condenser and evaporator) are similar in construction and purpose: heat is transferred from a fluid inside the tube to another fluid on the outside of the tube. From the compressor, the hot, high-pressure gas travels through the discharge line into the condenser. The main aim of this study is to understand the impact of a refrigerant mixture with components having different boiling points on condenser design, where condensation takes place on the shell side of the tubes.

1.3 Condenser

The condenser is the part of the system where the heat is removed from the working fluid, thus causing it, as the name implies, to condense. An everyday example of condensation is a container of cold water left outside on a hot summer afternoon. Since

the surface of the container is cooler than the air that surrounds it, water begins to leave the air and form drops on the container. As the water condenses from the air onto the surface of the container, it loses energy and, therefore, cools. In the air conditioning system, as the hot gas travels through the condenser, it is cooled by the coolant flowing inside tubes. As the hot gas refrigerant cools, drops of liquid refrigerant form on the tubes. Eventually, when the gas reaches the end of the condenser, it has condensed completely, that is, only liquid refrigerant is present. Just like the water condensing onto the surface of the container of cool water, the refrigerant has lost some of its energy and cooled.

1.4 Shell and tube condenser

The condensation of vapour is a frequent and essential part of many industrial processes. In the chemical industry, particularly, the condensation of vapour mixtures is at the heart of the industrial processes. A condenser is simply a device which directs flow paths in such a way that two streams are brought into thermal contact through a conducting wall, while being kept physically separate. Shell-and-tube heat exchangers are the most widely used type. This thermally conductive wall is the tube in shell-and-tube heat exchangers. A shell-and-tube heat exchanger consists of several tubes enclosed in a shell. One fluid flows through the tubes while the other fluid is conducted through the shell. The relatively thin-walled tubes, selected primarily for heat transfer efficiency, become the critical component in condensers and other heat exchangers, and must perform well over long periods of time under sometimes very difficult operating conditions (see figure 1).

1.5 Working fluids

Any chemical compound in principle can act as a refrigerant, provided it has a significant vapour pressure, is intrinsically stable over the range of temperatures it will experience in operation, and is compatible with the construction material and the lubricant. Since leakage from the systems is unavoidable, except for small hermetic-type systems, it has to be non-toxic, in several applications also non-flammable, and must not degrade the environment. Since no single compound fulfils all the above-mentioned conditions a choice has to be made, depending on the legislation, the economy, and the applications.

A number of working fluids are identified that meet the initial requirement of zero Ozone Depletion Potential (ODP) and these include R32, R134a, R125 and R143a etc. In Table1, some of these fluids are listed together with information about their physicochemical properties.

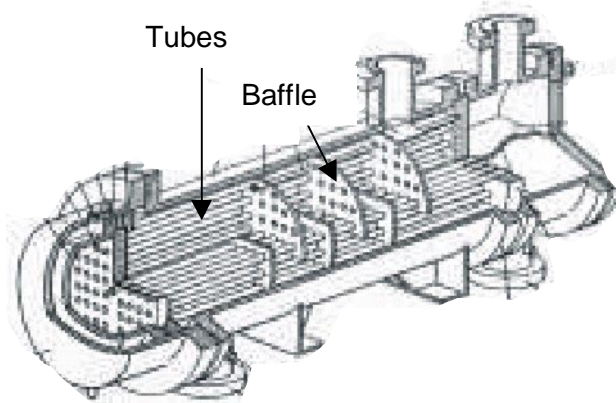


Figure 1: Tube layout in tube and shell condenser.

Table 1: Properties of some refrigerants

	R22	R32	R125	R134a	R407C(mixture)
Chemical Formula	CHClF_2	CH_2F_2	CF_3CHF_2	$\text{CF}_3\text{CH}_2\text{F}$	R32/R125/R134a 52/25/23%
Molecular Weight (g/mol)	86.47	52.02	120.02	102.03	86.20
Global Warming Potential (100 yr.)	1500	650	2800	1300	1530
Working Range ¹ (°C)	-41/63	-52/42	-48/51	-26/79	-44/57 (bubble point) -37/61 (dew point)
Liquid Density [kg/m^3] (273.15K)	1282	1055	1320	1295	1237

¹Temperatures corresponding to 0.1 MPa and 2.6MPa respectively.

Since no single fluid meets all the criteria as a replacement for R22, blends of these fluids are considered. A blend of R32, R125 and R134a, a zeotropic mixture named R407C, has proved to be a selective replacement for R22. It can be used in the existing systems after some minor changes. However, before using the mixture in a refrigeration machine, an optimization study of the complete cycle is required.

1.6 Consequences of zeotropic mixtures in condensers (literature review)

When a replacement of R22 with R407C in an R22-machine was carried out, a severe drop in condenser performance was observed [14], by almost 70% compared to R22 at lower effect. Similar reduction of heat transfer coefficient was observed [36], when the temperature difference between the cooled wall and the gas vapour was small. Hijikata et al. [20] studied the free convective condensation of binary vapours of R113/R11 and

R113/R114. At high temperature difference (ΔT) between the cold wall and the gas temperature, the result for R113/R11 tended to the Nusselt solution. However, at low ΔT the reduction in heat transfer coefficient with increased concentration of R11 was smaller than for the similar change of concentration of R114 in the R113/R114 mixture.

Murphy et al. [31] studied the forced convective condensation of R114/R12 mixture on finned tubes. The results showed that even low concentration of R12 reduces the heat transfer coefficient significantly. A reduction in heat transfer coefficient of the order of 55% was observed for 5% R12, due to additional transport resistance caused by the preferential concentration of more volatile component. Hijikata et al. [17,18,19] studied systematically the forced convective condensation of binary mixture of R113/R114 on smooth, as well as horizontally and vertically finned tubes. Very similar results were obtained. At low Reynolds number and low ΔT , the reduction in heat transfer coefficient was higher than at high temperature difference. At higher Reynolds number even low temperature difference gave less reduction in heat transfer coefficient. Very similar observations were made by Nozu et al. [32].

1.7 Aim of this thesis

Replacement of the conventional refrigerant R22 is one of the urgent issues to be solved within the scheduled time frame of the international regulations of refrigerants. New hydro-fluorocarbon (HFC) refrigerants without any chlorine are proposed to be applied in refrigeration, heat pumps and air-conditioning systems. R407C is one of the potential replacements for R22, but according to measurements a very large decrease in condenser overall heat transfer coefficient was observed for R407C compared to R22 [14]. This study led to the fact that the major focus of a research project carried out in cooperation with Sabroe Refrigeration in Norrköping, Sweden, was shifted towards finding causes for and countermeasures against such performance drops.

The aim of this thesis is to increase the knowledge about the impacts of the replacement of R22 by R407C, or similar zeotropic mixtures with glide, on the condenser design. The objectives of this work may be summarized as:

- To identify the main differences between the condensation of a mixture with components having different boiling points and that of a pure fluid.
- To learn how different assumptions about mixing behaviour and flow patterns affect the calculated rate of condensation.
- To investigate whether modifications of the condenser geometry built originally for R22 can lead to higher condensation rates for R407C.

For these purposes a computer program taking into account the effects of different physicochemical properties of the gas vapours was developed. In the second phase of

the present work, the computer program developed in the first phase was integrated with a CFD (Computational Fluid Dynamics) program to quantify the effects of flow pattern and the geometrical modifications on the condenser design.

1.8 Program Climate 21

This project has been carried out within the framework of the research programme Climate 21. The research program Climate 21 is jointly financed by industry and initially by the Swedish National Board for Industrial and Technical Development, NUTEK. NUTEK's role is now taken over by the Swedish National Energy Administration. It is a continuation and a widening of a former program called "Alternative Refrigerants".

Climate 21 is focused on energy efficiency in heat pumps, air conditioning and refrigeration systems. The program will cover the whole technical chain from components to units and systems within the area of heat pumps and refrigerating systems. The objective of the program is to strengthen the Swedish industry on a long-term basis by exchange and transfer of knowledge between the industry and the universities.

1.9 Organization of the thesis

The thesis is divided into five chapters. The first chapter introduces the basics of the vapour-compression machine, shell-and-tube condenser, and working fluids used in these machines.

The mathematical interpretation of the physical phenomena taking place in condensation processes is presented in Chapter 2. In Chapter 2, a literature review regarding the condensation of multicomponent mixtures is also presented. Chapter 3 introduces Computational Fluid Dynamics (CFD), a computational technique widely used today when there is any kind of fluid flow involved.

Results and discussions about the parameters that affect the rate of condensation in a shell-and-tube condenser are presented in Chapter 4.

2. Important concepts

2.1 Condensation of zeotropic mixtures

Condensation of a zeotropic mixture differs from that of a pure fluid in two ways. First, the temperature at which condensation occurs is not uniform throughout the condenser and, second, effects of mass transfer resistance are introduced. As the heavier component is more liable to condense first, the remaining vapour mixture has a lower bubble-point, thus causing the equilibrium temperature to fall. A practical consequence will be reduced temperature difference between the coolant and the condensing side, with a corresponding reduction in local heat transfer.

The preferential condensation of the heavier component results in accumulation of the lighter component at the interface, thus making a layer through which heavier or less volatile components have to diffuse. This resistance to the transfer of heavier components, caused by the accumulation of lighter components at the interface, is called the mass transfer resistance. Furthermore, the kind of condensation can be divided into two types: differential and integral. In the integral kind of condensation, the condensate and the gas vapour are assumed to be in intimate contact, as they flow through the condenser and the system composition remains constant. In the differential type, condensate, once formed, is separated from the gas. This kind of separation can take place due to condensate holdup or if the condensate separates from the surface after it is formed. There is no exact evidence for what kind of condensation actually occurs. Integral and differential condensations are described in more detail in Section 2.3, “Condensation curves”.

Design of a condenser for zeotropic mixtures requires, besides low-pressure drop, that the gas and condensate should follow the same path through the condenser. Gas/condensate separation or condensate holdups in the condenser can lead to the differential kind of condensation, which means low temperature driving force and, in some cases, uncondensed vapour. There are two kinds of approximate methods to describe the condensation of multicomponent mixtures. The first kind is a simple

method proposed by Silver, where the equilibrium curve is assumed to be known, and the second is based upon film theory.

2.1.1 Silver's Method

The method is based on calculating an effective vapour-side heat transfer coefficient such that the overall heat transfer coefficient can be written as

$$\frac{1}{U} = \frac{1}{h_c} + r + \frac{1}{h_{eff}} \quad (1)$$

where h_c is the coolant-side heat transfer coefficient and r is the thermal resistance of the tube wall including fouling on the tube surface. The method to calculate the effective heat transfer coefficient h_{eff} has been devised by Silver, Bell and Ghally. In this method h_{eff} is given as

$$\frac{1}{h_{eff}} = \frac{1}{h_L} + \frac{z_g}{h_g} \quad (2)$$

where h_L is the heat transfer coefficient for the condensate layer and h_g is the gas-phase heat transfer coefficient. The parameter z_g is given as

$$z_g = x_g c_{pg} \frac{dT_g}{dh_m} \quad (3)$$

where x_g is the gas-vapour phase mass flow fraction, c_{pg} is the specific heat for the gas-vapour mixture and h_m the enthalpy of the gas-liquid mixture. The parameter z_g is usually calculated by assuming equilibrium between the gas bulk and the liquid. This assumption can yield too small as well as too large values for U [40]. For this reason, one has developed more precise methods to be discussed in the following sections.

2.1.2 Multicomponent condensation based on film theory

The film model was proposed by Colburn & Hougen [11] and Colburn & Drew [12] for binary vapour mixture condensation. The model was based, first, on the assumption that at the vapour-condensate interface the compositions of the two phases are the equilibrium compositions at the interface temperature and the system pressure. Second, they assumed that the vapour-phase resistance to both the heat and mass transfer lies in a stagnant film adjacent to the vapour condensate interface, shown in Fig. 2. The procedure proposed by [12] is to equate by trial and error the heat transferred through the condensate layer, the tube wall and the cooling water film with the sum of the sensible heat from the cooling of the uncondensed gas and the latent heat of the condensing vapour flux, which requires knowledge of the local interface temperature.

Extension of the above methods is not straightforward. Multicomponent mass transfer is complicated by the possibility of diffusional interaction, where the rate of transfer of each individual species can depend upon all the independent concentration gradients in

the system. Thus, in multicomponent systems it is possible to obtain various interaction phenomena ([37], [39]) such as osmotic diffusion (transport of a species in the absence of its concentration gradient), diffusion barrier (no transport of component even though a concentration gradient exists) and reverse diffusion (diffusion of a species against its gradient).

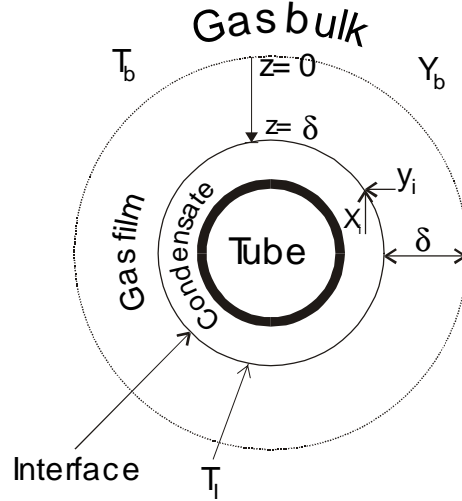


Figure 2: The film model.

2.1.3 Gas-phase mass transport

The species transport under isobaric and isothermal conditions for an ideal gas mixture can be expressed with the help of the Stefan-Maxwell equation:

$$\frac{dy_i}{dz} = \sum_{\substack{j=1 \\ j \neq i}}^K \frac{y_i N_j - y_j N_i}{CD_{ij}} \quad (4)$$

where N_i are the molar fluxes toward the condensate surface, and D_{ij} is the binary diffusion coefficient of component ‘‘i’’ in component ‘‘j’’. These coefficients are estimated from [13]. If δ is the gas film thickness as shown in Fig. 2, a dimensionless distance coordinate $\eta=z / \delta$ yields

$$\frac{dy_i}{d\eta} = \sum_{\substack{j=1 \\ j \neq i}}^K \frac{y_i N_j - y_j N_i}{\beta_{ij}} \quad i = [1, K-1] \quad (5)$$

where β_{ij} ($\text{mol}/\text{m}^2\text{s}$) are binary mass transfer coefficients corresponding to zero flux conditions and can be expressed as [10]

$$\beta_{ij} = C \frac{D_{ij}}{\delta} \quad (6)$$

where C is the gas molar density $C = \frac{p}{RT}$.

Only K-1 equations (5) are needed to model the transport of K species, since the composition gradient of the Kth component can be written as

$$\frac{dy_K}{d\eta} = -\sum_{i=1}^{K-1} \frac{dy_i}{d\eta} \quad (7)$$

Equation (2) for K-1 components can be written in matrix form as

$$\frac{d\mathbf{y}}{d\eta} = \mathbf{A}\mathbf{y} + \boldsymbol{\xi} \quad (8)$$

where \mathbf{y} and $\boldsymbol{\xi}$ are column matrices of the order (K-1) and \mathbf{A} is a square matrix of the order K-1. This set of linear differential equations can be solved with boundary conditions (at $\eta = 0$, i.e. at the bulk gas boundary $y=y_b$).

Krishna and Standard [28] have developed a mathematical procedure to solve this equation system, taking into account the dependence of the β_{ij} on finite mass transfer rates N_i .

2.2 Energy balances and heat transfer rate relations

If the gas is superheated, sensible heat q_g transferred from the gas to the interface can be described as

$$q_g = h_g^* (T_b - T_I) \quad (9)$$

where h_g^* is the gas-phase heat transfer coefficient corrected for the mass transfer effects. This correction is needed since the heat flux, which arrives at the interface as sensible heat, comes from two sources: the cooling of the main gas stream, and the cooling of the condensing mass flux N_{tot} from the bulk-gas temperature T_b to the interface temperature T_I . As pointed out by Ackerman [1], h_g^* can be calculated:

$$h_g^* = h_g \frac{\theta}{1 - e^{-\theta}} \quad (10)$$

where

$$\theta = \frac{\sum_i N_i C_{p_i}}{h_g} \quad (11)$$

Now the temperature change in the main bulk gas stream can be written as

$$(G/M_m)C_{p_m} \frac{dT_b}{dA_o} = -q_g + \sum_{i=1}^K N_i C_{p_i} (T_b - T_i) \quad (12)$$

where G is the mass flow of the mean gas stream and dT_b is change in bulk gas temperature. Equations (9,10,11 and 12) give

$$(G/M_m)C_{p_m} \frac{dT_b}{dA_o} = -h_g \frac{\theta}{e^\theta - 1} (T_b - T_i) \quad (13)$$

The latent heat of the condensing vapour and sensible heat from the bulk gas are transferred from the gas/condensate interface to the coolant by conduction:

$$dQ_L = h_L (T_i - T_c) dA_o = \pm (m_c / M_c) C_{p_c} \Delta T_c \quad (14)$$

where h_L indicates the heat transfer coefficient from the condensate surface to the coolant, dA_o is the surface area element of the interface, T_i its temperature, T_c the local temperature of the coolant and m_c is the coolant flow rate (kg/s).

A heat balance over the gas/condensate interface, or the overall heat balance, can be written as

$$h_L (T_i - T_c) = h_g^* (T_b - T_i) + h_{fg} \sum_{i=1}^K N_i \quad (15)$$

2.3 Condensation curves

Condensation of a component occurs when the wall temperature is slightly below its saturation temperature. Since the mass diffusion and convection processes in mixtures occur simultaneously, the interfacial temperature or the saturation temperature depends upon local concentration and pressure of the gas and the condensate. The relative paths of the gas-vapour and the condensate are important to determine the compositions.

In the literature, two different views exist regarding the mixing in the condensate film or the type of condensation curve. The first is the integral view, i.e. the gas and the condensate are in intimate contact with each other, and the second, the differential view, occurs e.g. when the condensed phase formed is immediately removed from the system. Most of the computer programs used for designing shell-and-tube condensers are based upon the integral condensation curve. Which kind of condensation takes place in

condensers with complicated geometry as of shell-and-tube is difficult to say. The reality should be somewhere between these two extremes.

The differential kind of condensation is illustrated in Fig. 3. The condensate leaves the system immediately as it is formed. Since the less volatile components are more liable to condense out first, the remaining gas bulk will have higher concentration of lighter or more volatile components. Higher concentration of lighter components will lead to lower condensation temperatures.

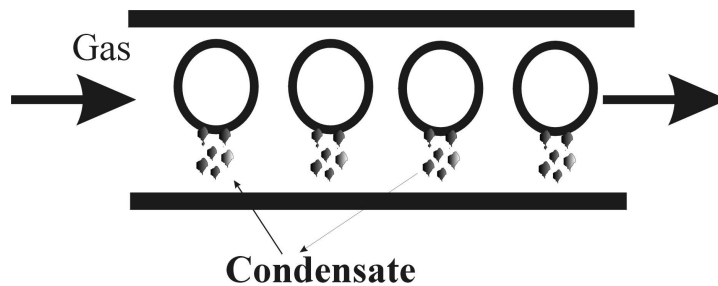


Figure 3: Differential condensation. Condensate from each tube is separated, and the gas flows to the next tube.

Contrary to the above, if the condensate is formed and the gas bulk remains in intimate contact, the concentration of the lighter components will increase, but not in the same fashion as in the case of differential condensation. This kind of condensation curve is called the integral condensation curve. The phenomenon of integral condensation is illustrated in Fig. 4.

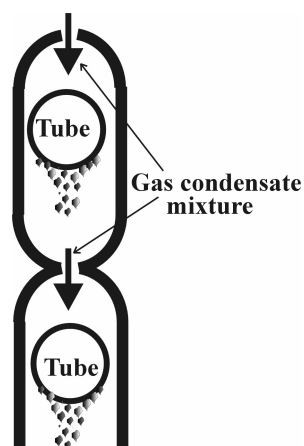


Figure 4: Integral condensation. Gas and condensate from each tube are assumed to be well mixed.

To illustrate the practical significance of these two extremes, consider a binary mixture of R32 and R134a. R32 is the lighter component in the mixture. It enters initially in the gas phase with a mole fraction $y=0.5$. Then, due to mass transfer resistance in the gas phase, the gas phase mole fraction at the interphase on the first tube row, y_1 , becomes 0.55. Starting from this point, Fig. 5 illustrates the condensation process over a tube bank with a total of 24 tube rows. The numbers on the bubble point line indicate the tube row number. The first condensate drop that appears on the first tube row has a molar fraction equal to x_1 and temperature T_1 .

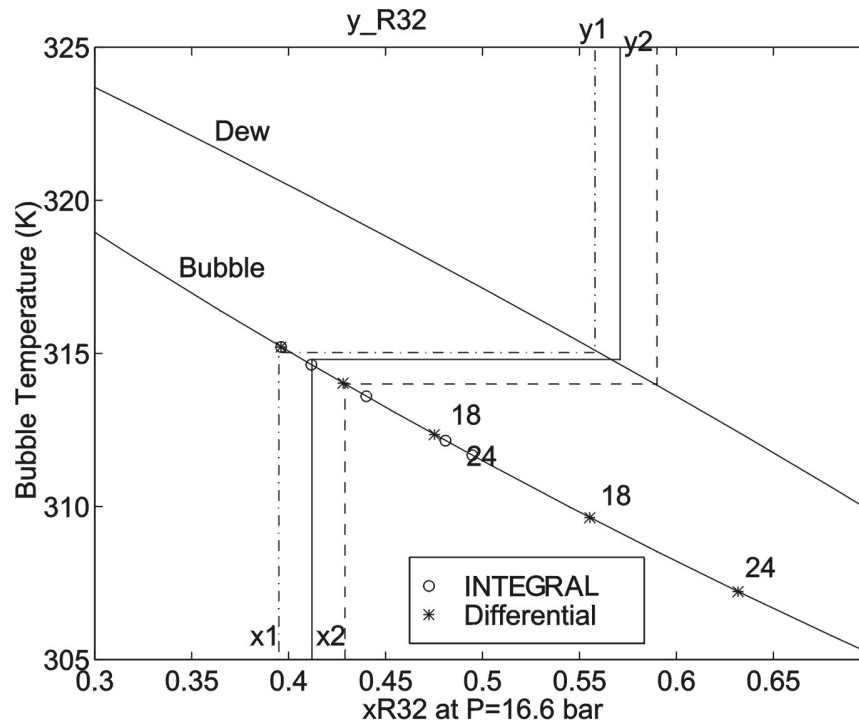


Figure 5: The type of condensation curve and the variation of condensation temperature for 50-50 (molar%) R32-R134a mixture.

Now suppose that the condensate formed at the first tube leaves the system as it is formed. Since condensate at the first tube row has a higher molar fraction of R134a, the gas bulk surroundings would have higher concentration of R32. This means that the condensate on the second row will be in equilibrium with the gas correspondingly having higher fraction of R32. In this way, if the condensate leaves the system at each tube row, the molar fraction of R32 in the gas bulk increases, and that would lead to lower condensation temperatures as shown in Fig. 5, 307.2K, when all the gas bulk has condensed.

Now contrary to the above, suppose that the condensate from the first row mixes with the condensate formed at the second tube row as illustrated in Fig. 4. The equilibrium leads now to a higher temperature, due to the fact that the condensate from the first tube

row, having a higher molar fraction of R134a, is not separated from the system. As shown in Fig. 5, when all the gas phase is condensed, the condensation temperature in the case of integral condensation is 311.6K, as compared to 307.2K in the case of differential condensation.

The influence of the gas phase mass transfer can be seen by comparing the interphase temperature T_1 obtained for $y_1=0.55$ (about 315 K) with the one obtained assuming no resistance, i.e. $y_1=0.50$, which would give T_1 about 317 K.

2.4 Heat transfer coefficient in condensate layer

Development of correlations for the prediction of heat transfer coefficients for the condensate film has been a matter of intensive research. In the literature, various simple and complicated methods exist to predict the heat transfer coefficient ([21], [22], [24], [25], [4], [5], [9], [38]). The old models based on Nusselt's theory [33] assume that condensate drainage is only due to gravity. In the case of low surface tension fluids according to [4,5], gravity drainage is in fact more important than drainage due to surface tension. However, a short analysis is given in the subsequent section about the effect of surface tension.

For a single, plane horizontal tube, and with laminar film condensation, the classical expression for the heat transfer coefficient was developed by Nusselt [33]:

$$\bar{h}_l = 0.725 \left(\frac{k_l^3 \rho_l^2 g h_{fg}}{\mu_l} \right)^{1/4} \left(\frac{1}{(T_i - T_w)} \right)^{1/4} \left(\frac{1}{d_r} \right)^{1/4} \quad (16)$$

It was assumed that the effect of vapour shear is insignificant, the condensate drains only due to gravity, and the heat transfer in the film is only due to conduction.

Today, low-fin tubes are commonly used in shell-and-tube condensers in refrigeration and air conditioning. Use of externally finned tubes has proved to be a highly effective means of enhancing film condensation and heat transfer on horizontal tubes. The first theoretical model to predict heat transfer on finned tubes, where condensate drainage is only due to gravity, was proposed by Beatty and Katz [2]. The model is based on adding up the contributions to heat transfer of the fin flanks and the tube surface between the fins, as shown in Fig. 6:

$$h_l = h_u \frac{A_u}{A_o} + \eta_f h_f \frac{A_f}{A_o} \quad (17)$$

where η_f represents the fin efficiency and A_o is the effective area, i.e. the sum of the areas of the fins A_f and the bare tube A_u as shown in Fig. 6; h_u is the Nusselt coefficient for horizontal tubes and h_f stands for the Nusselt's coefficient for vertical plate.

$$h_u = 0.725 \left(\frac{k_l^3 \rho_l^2 g h_{fg}}{\mu_l (T_l - T_w) d_r} \right)^{1/4} \quad (18)$$

$$h_f = 0.943 \left(\frac{k_l^3 \rho_l^2 g h_{fg}}{\mu_l (T_l - T_w) H_f} \right)^{1/4} \quad (19)$$

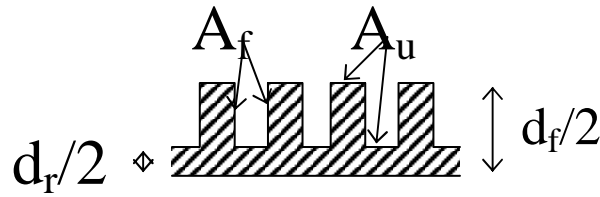


Figure 6: Model of Beatty-Katz tube.

After inserting the expressions for h_u and h_f , they arrived at the following expression:

$$h_l = 0.689 \left[\frac{k_l^3 \rho_l^2 g h_{fg}}{\mu_l (T_l - T_w) d_{eq}} \right]^{1/4} \quad (20)$$

where d_{eq} is an equivalent diameter that can be expressed as

$$\left\{ \frac{1}{d_{eq}} \right\}^{1/4} = \frac{0.943}{0.725} \eta_f \frac{A_f}{A_o} \frac{1}{H_f^{1/4}} + \frac{A_u}{A_o} \frac{1}{d_r^{1/4}} \quad (21)$$

where H_f is the mean effective height of a fin,

$$H_f = \frac{\pi}{4d_f} (d_f^2 - d_r^2) \quad (22)$$

The adjustment of the theoretical value 0.725 in equation (20) to 0.689 correlated their experimental data within $\pm 10\%$. According to [22], the model of Beatty and Katz predicts data for R22 within $\pm 20\%$.

Equations (16) and (20) can be expressed in terms of condensing mass flux by replacing the temperature difference $(T_l - T_w)$ with a heat balance over the tube:

$$h_{fg}\Gamma = \bar{h}_l(T_i - T_w)\pi d_r \quad (23)$$

where Γ (mol/ms) is the condensing mass flux per unit tube length. Using (23), equation (16) in terms of condensing mass flux for a smooth tube can be written as

$$\frac{\bar{h}_l}{k_l} \left[\frac{\mu_l^2}{\rho_l(\rho_l - \rho_g)g} \right] = 1.51 \left(\frac{4\Gamma}{\mu_l} \right)^{\frac{1}{3}} \quad (24)$$

A similar expression for the heat transfer coefficient for a finned tube, equation (20), can be written as

$$h_l = 0.645 \left(\frac{1}{d_{eq}} \right)^{1/3} (A_o)^{1/3} \bar{h}_l \quad (25)$$

2.5 Effect of inundation

Condensation coefficients for heat transfer depend on the thickness and properties of the condensate film on the surface. In the case of condensation in tube banks, the film thickness on the lower tubes increases due to falling condensate. The heat transfer coefficient for tube banks with negligible vapour shear is often expressed as [27]

$$\frac{h_{lN}}{h_{l1}} = N^{-1/s} \quad (26)$$

where h_{lN} and h_{l1} are the heat transfer coefficients for the N^{th} row and the top row respectively. The values of ‘‘s’’, proposed by Nusselt [33] and Kern [27] for smooth tubes, are equal to 4 and 6 respectively. According to Ph. Blanc [3], at low heat fluxes the measured results for the similar tubes are in close agreement with that of the equation proposed by Kern [27]. Grant and Osment [16] expressed the effect of condensate inundation in terms of the condensate fluxes:

$$h_{lN} = h_{l1} \left\{ \frac{\Gamma_N}{\gamma_N} \right\}^{-0.223} \quad (27)$$

where Γ_N is condensate drainage from the N^{th} tube and γ_N is the condensate generated at that tube. According to Butterworth [7], equation (26) is in close agreement with equation (27).

2.5.1 Effect of surface tension on film condensation

As mentioned before, the Beatty and Katz model [2] does not consider the effect of surface tension. The surface tension effect on the behaviour of condensate is composed of two factors. The first is reduction of the condensate film thickness on the fin surface at the upper part of the tube, which leads to enhanced heat transfer. The second is

retention of the condensate between the fins at the lower part of the tube, which leads to a decrease in the effective surface area. Good agreement of the Beatty and Katz model, according to [38], is because of compensating errors. The model underpredicts the heat transfer coefficient at the fin surface but also neglects the flooded region on the tube bottom, which leads to overprediction of the surface area.

According to [24,4], the flooding angle, i.e. the angle measured from the top of tube below which the interfin space becomes full of retained condensate, can be calculated as

$$\phi_f = \cos^{-1} \left(\frac{2\sigma \cos \theta}{\rho_l g d_o s} - 1 \right) \quad (28)$$

where σ is the surface tension, and d_o is the diameter of the tube over the fins.

For the tube used in this work about 8% of the surface area was found to be filled with retained condensate. However, as can be seen, the flooding angle for a specific tube geometry is dependent upon the surface tension of the fluid.

2.5.2 Effect of vapour shear

If the vapour velocities are significant, as in the case of surface condensers, the large interface shear forces on the condensate film could subsequently alter the condensate flow around the tube. But [15], [29] and [21] have shown that the effect of vapour velocity on finned tubes is not so significant. The vapour velocities in the case studied in this work are much lower than those considered by [15], [21]. We can say that the effect of vapour shear would be insignificant.

2.6 Heat transfer coefficient and enhancement ratio

In the literature, the performance of a finned tube compared to that of a plane tube is often represented as an enhancement ratio at constant ΔT , or at constant heat flux (q). It is important to remember that the enhancement ratio at constant ΔT , equation (30), is not the same as at constant heat flux, equation (29):

$$\mathcal{E}_q = \frac{h_{finned}}{h_{plane}} \Big|_q = \frac{(q/\Delta T)_{finned}}{(q/\Delta T)_{plane}} \Big|_q = \frac{\Delta T_{plane}}{\Delta T_{finned}} \quad (29)$$

or

$$\mathcal{E}_{\Delta T} = \frac{h_{finned}}{h_{plane}} \Big|_{\Delta T} = \frac{(q/\Delta T)_{finned}}{(q/\Delta T)_{plane}} \Big|_{\Delta T} = \frac{q_{finned}}{q_{plane}} \quad (30)$$

where the heat flux and the heat transfer coefficient are based on the smooth tube surface area. However, experiment has shown that in condensation on plane and low-

finned tubes the heat flux and condensation temperature difference are generally not far from $q \propto \Delta T^{3/4}$ (as in the Nusselt theory for a plane tube). If this is true, the relation between the enhancement ratios at constant heat flux and constant temperature difference can be written as

$$\mathcal{E}_q = (\mathcal{E}_{\Delta T})^{-4/3} \quad (31)$$

3. CFD and the condenser design

3.1 Introduction

A common feature of most condensers is the provision of by-pass and regenerative lanes to facilitate the access of vapours to the lower part of the condenser without excessive pressure drops. The actual path of vapours in tube banks must therefore be relatively complex. Models based on assumptions like the one made in Paper I may overestimate the heat transfer. The model in the paper was based on the assumptions that:

1. flow in the condenser is vertically downwards;
2. velocity and composition of the components are constant along a horizontal plane.

For improvement of the condenser design, and to get insight into the interactions of complex physical phenomena taking place around a tube in a shell-and-tube condenser, knowledge about the flow pattern is significant. Traditionally, experimental and theoretical methods have been used to obtain the design information on the transport properties of equipment. Existing published methods for the design of condensation in tube bundles do not represent the effect of gas flow and its effect on condensation rates. The complicated geometry makes such studies, if not impossible, too expensive. With the emergence of high-performance computer facilities, a new method based on a numerical approach has become available. Such a computational approach will not, however, completely replace the experimental testing but rather reduce the dependence on those activities. In the second phase of this work such a Computational Fluid Dynamics (CFD) package, integrated with the computer code developed in the first phase of the project, has been used. This made it possible to visualize the local velocity, temperature, pressure and concentration fields.

3.2 What is CFD modelling?

CFD modelling is a computational technique that solves the Navier-Stokes equations together with the enthalpy equation and species equations if the fluid is a mixture. The equations are solved by numerical approximation methods, either a Finite Difference Method (FDM) or a Finite Element Method (FEM). In either case, the solution domain is divided into computational cells. In the present work, the domain or the condenser geometry, shown in is divided into rectangular cells based on the body-fitted coordinate (BFC) option, which enables the grid to be smoothly fitted to the non-regular physical boundaries. The grid around a tube is shown in Fig. 7.

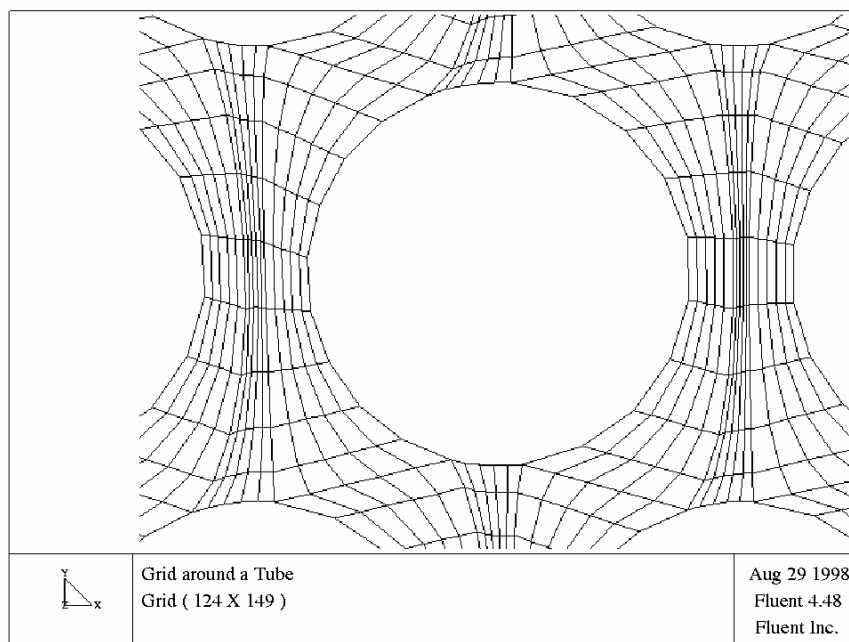


Figure 7: The computational mesh around the tube surface.

The CFD approach can be used in any investigation where fluid flow and related transport phenomena are involved. Although CFD codes can handle most of the physical phenomena occurring in condensation processes quite successfully, computer limitations require approximations or simplifications. Some detail about the simplifications made in this work is given in the next section.

3.2.1 Choice of the CFD program

A pilot study was conducted to find a CFD program that suited our needs. Our primary aim was to find a program that

- could handle heat and mass transfer
- was easy to modify with user subroutines.

Furthermore, to apply the rate of condensation around different tubes, the information about gas concentration and areas of cells should be easily accessible.

Although there are many CFD programs available on the market, few of them are general-purpose programs. Most of the CFD programs were developed for solving problems originating in the nuclear power plants industry. We found that CFX, FIDAP and FLUENT (structured) were the only programs that could be of use regarding heat and mass transfer and the applications of user subroutines. It is impossible to say which program is good or bad. We decided for FLUENT (structured) after a few weeks of training with FIDAP.

FLUENT (structured) is based on finite volume methods, i.e. the calculation domain is divided into cells of finite volumes. All these cells or volumes are stored in an array. Each element in this array contains information about the geometrical and physical quantities and the type of cell (Live, Dead or any other kind). This information is quite easy to access but sometimes it needs some manipulations. As an example: the area of the cells is stored as a projection of the area onto the I-J axes.

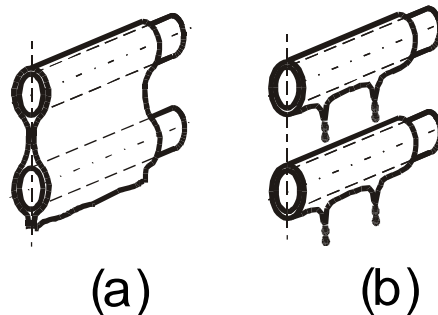


Figure 8: Types of condensate film drainage, (a) sheet-like, (b) drops.

3.3 Simplifying assumptions

Since shell-and-tube condensers, taking two-phase flow, heat and mass transfer as well as complete geometry into account, require excessive computing capacity, we have chosen to make the following simplifications:

1. The problem is solved as one-phase with condensing component fluxes as boundary condition. Only the gasbulk is simulated with the CFD program [7] and the condensation processes around each tube are modelled with User Defined Subroutines linked to the main CFD program. Tube walls in the CFD program are treated as gas/condensate interface. Gas-bulk temperature, concentration and velocity from

the CFD program are passed to the User Defined Subroutine, and the calculated condensing massfluxes and the condensation temperature in the Subroutine are specified as boundary conditions in the CFD model. The whole procedure is an iterative loop, where boundary conditions are modified based on the bulk conditions in each sub-loop.

This assumption is needed, since modelling the mass transport in the CFD program requires a very fine mesh in the near-wall regions. The mesh size in these regions should be less than the gas-film thickness; otherwise, numerical discretization schemes would lead to negative concentration at the tube surface.

The “transfer area” error introduced by neglecting the thickness of the condensate layer is marginal, since it for the conditions investigated here can, according to Nusselt [33], be estimated to be between 0.04 and 0.3 mm.

2. The model presented in this work is 2-dimensional, mainly due to the limited computational capacity we have and to get reasonable computational times. The present model can be seen as meaning that the gas inlet is like a strip at the top of the condenser having length equal to tube length, and the mass transfer in the direction along the tube length is ignored. Generally, in practice the gas inlet is located at the middle of the condenser and slightly tilted.
3. Equal condensation rate around the tube surface was assumed, even though we are aware of the fact that the local calculation around the tube surface, for both heat and mass transfer, probably would give better estimates of the condensing fluxes. These simplifications are needed, first, because the correlations used to calculate the heat and mass transport are based on average gas flow and give average values, and second, to get reasonably short computational time.
4. The obstruction to the gas flow due to condensate film is not taken into account. The only obstruction to the gas flow that is taken into account is due to tubes. However, if the condensate flows as a film in the tube bank as shown in Fig. 8a, which could be the case for lower tube rows, obstruction to the gas flow due to condensate film should be taken into account. In the present case the condensate flow is assumed as droplets (shown in Fig. 8b) falling vertically downwards on the lower tubes.
5. The drag due to falling condensate on the gas film might influence the mass transfer characteristic in the gas film. However, taking into consideration such phenomena would require a very detailed modelling of the near-wall or near-condensate regions.
6. It was found that there were convergence problems when assuming laminar flow. The k- ϵ model was therefore used to describe the turbulence. The results showed that the flow was laminar except in a region around the impingement plate.

4. Results and summary of papers

Summaries of the results presented in Paper I and Paper II are given below. Paper I covers the simulations done with the help of the computer program developed at the department, and the comparison of the simulation results with experimental data. The main aim of Paper I is to find out the possible reasons for the performance deterioration of a shell-and-tube condenser when a zeotropic mixture R407C is used as the working fluid. The results presented in Paper I are based on a pre-assumed flow field. It was assumed that the gas bulk flows directly downward and the velocity of gas is uniform along a horizontal plane. In Paper II, the assumption of uniform vertical downward flow was released, and instead the flow field is simulated in a CFD program linked to the computer program developed in the first phase of the project.

4.1 [Paper I: “Reasons for drop in shell-and-tube condenser performance when replacing R22 with R407C”](#)

4.1.1 Comparison of condenser performance

Generally, the performance of a heat exchanger is compared in terms of an overall heat transfer coefficient. The overall heat transfer coefficient may be calculated as

$$U = \frac{Q}{A\Delta T_{\ln}}$$

where Q stands for the total transferred effect, A the total area and ΔT_{\ln} the mean logarithmic temperature difference. This kind of comparison is valid only for co- and counter-current flow and when the $W \cdot C_p$, the product of mass flow and heat capacity for the fluids, is constant. In simulations, area needed for the condensation is calculated, which do not need to be equal to the total area of the condenser.

Since neither of the assumptions mentioned above holds for the condenser investigated in this work, two alternative ways to compare the performance are discussed. Fig. I:4 (Fig. 4, Paper I) shows the comparison of the measured overall heat transfer coefficient (U_{meas}) and the calculated U_{calc} . It was assumed that:

1. the Logarithmic Mean Temperature Difference (LMTD) for cross flow can be expressed as the average of the LMTDs for the co- and counter-currents respectively;
2. the average overall heat transfer coefficient $\langle U_{\text{calc}} \rangle$ for the total condenser-area A can be obtained as $\langle U_{\text{calc}} \rangle = U_{\text{calc}} \cdot A_{\text{calc}} / A$, where U_{calc} is the average value for the area needed for total condensation, A_{calc} .

In Fig. I:2, the condenser performance is compared in terms of a correction factor. The heat transfer coefficient h_L (Equation 24), is multiplied by a correction factor to get the same outlet conditions as in experiments. A value of the correction factor less than one indicates that the simulation program overpredicts the heat transfer rate, and a value greater than one indicates underprediction.

4.1.2 Performance comparison of pure (R22) and mixed working fluid (R407C)

In Fig. I:2 the comparison of the overall heat transfer coefficient, in terms of correction factor, for the pure fluid R22 and a zeotropic mixture R407C is made. As can be seen, the simulation program predicts an almost constant value of the correction factor (0.86) in the case of R22. The correction factor for R407C decreases to 0.25 from 0.65 when the effect changes from 735kW to 250kW, which means that the simulation program overpredicts the heat transfer by 35% at 735kW condenser load and by 75% when the condenser load is 250kW.

The next question is what causes such different behaviour of R407C compared to R22. Both R22 and R407C have very similar thermal properties and the only factor that is not taken into account is the mixing in the condensate layer, i.e. the kind of condensation. Results presented in figures are based on the assumption that the condensation is integral. Calculations were carried out for different values of integration ratio (ϕ) such that the correction factor for R407C is equal to that for R22. Results presented in Fig. I:5 show that the condenser performance in the case of R407C could be explained in terms of mixing in the condensate layer. A 15% differential condensation at lower condenser effect gives the same correction factor as for R22.

4.2 [Paper II: “Influence of condenser design on flow pattern and performance of shell-and-tube condenser for zeotropic refrigerant mixture”](#)

The effects of geometrical modifications and flow pattern on condenser design for zeotropic, multicomponent mixtures are investigated in this paper. As discussed in Chapter 2, condensation of zeotropic mixtures differs from the condensation of pure

components due to two main reasons. The first reason is that the condensation is not isothermal, and the second reason is the resistance to mass transport. The temperature variation is discussed in section 2.3 in terms of the kind of condensation, i.e. differential or integral. Designers should try to approach the integral condensation curve, by avoiding segregation of the gas and the condensate.

Traditionally, condenser designs are based upon empirical information and pre-assumed flow fields. The designer arranges condenser tubes to give satisfactory performance. Shell-side by-pass is used to facilitate access of vapour to the lower region of the tube bank without excessive pressure drop. However, an excessive by-pass flow can lead to differential condensation, due to different flow paths of the gas and the condensate. Effects of decreasing the shell-side by-pass on condenser performance are shown in Fig. II:4 (Figure 4, Paper II).

An impingement plate opposite to the gas inlet is used to reduce tube erosion or vibrations. However, it may deflect the flow so that a significant amount of gas flows through the shell-side by-pass. The result can be that a significant part of the condenser remains ineffective, because gas bulk has to take a long path to reach the tubes in the middle of tube bank. The effects of using a porous impingement plate, such that about 50% of the inlet gas flows through it, are investigated in this article. Figures. 5, 6 and 7 in Paper II show the streamlines of the gas velocity for the base-case condenser configuration, and the one where the plate is changed to a porous plate respectively.

Use of baffled shells is common to increase the heat transfer by increasing gas velocities. Using baffled shells in the case of zeotropic mixtures can, however, have adverse effects on condenser performance, due to gas/condensate separation or the differential kind of condensation curve. The interface or the condensation temperatures profile for a baffled and an unbaffled shell is shown in Fig. II:3

Effects of these geometrical modifications are summed up in Fig. II:4. We can see that these geometrical modifications lead to increasing the rate of condensation by 15%.

From the present investigation, the following conclusions can be drawn:

1. Baffled shells leading to gas/condensate segregation should be discouraged.
2. Use of a porous impingement plate with a decreased shell-side by-pass leads to 15% higher condenser performance.

5. Conclusions and recommendations

5.1 Conclusions

In the first phase of this project, a comprehensive computer simulation program has been developed for the design of shell-and-tube condensers for pure as well as zeotropic mixtures. Two main differences that make the condensation of zeotropic mixtures different from the condensation of pure fluids are recognized. The first is the mass transport resistance, due to different propensity to condensation of different components in the mixture. The second is the mixing of the newly formed condensate on a particular tube with the condensate from the tubes situated above in a tube bank.

Based on the results presented in Paper I the following conclusions can be drawn:

1. The mixing in the condensate film explains the performance deterioration observed in experiments when replacing R22 with R407C.
2. Area needed for condensation increases by around 8% due to mass transfer resistance.

In the second phase of this project, fluid flow simulations are carried out, using a CFD program. Various geometrical modifications that lead to higher condenser performance are investigated. Approximations or assumptions made to simplify the CFD approach are discussed in the previous section. Results are compared to the base-case configuration, i.e. the “as it is” configuration. Regarding the effects of flow pattern, the following conclusions can be drawn:

1. Flow pattern has a very significant impact on condenser performance.
2. Decreasing the shell-side by-pass and replacing the impingement plate by a porous impingement plate increases the condenser performance by around 15%.

5.2 Recommendations

A number of simplifications and assumptions made in this work are listed in the above chapters. In this section, a few recommendations for removing some of these assumptions are given.

The concentration plots presented in Paper II illustrate the variation of R32, the most volatile component in the zeotropic mixture R407C. Since the condensation temperature is a function of the local pressure and the concentration, the condensation temperature would vary from tube row to tube row. To compare the experimental results with the simulated ones, local experimental measurements in the condenser would be needed. Measurements of at least water temperatures from each tube row would be of great help.

A 3-D simulation, which has not been performed because of limited computational capacity, would be needed to make the model more realistic regarding the flow pattern and mass transfer along the tube length.

Effects of surface enhancement on flow pattern are neglected in this work. Detailed CFD simulations are needed to understand how different surface enhancements influence multicomponent condensation.

6. Acknowledgements

I would like to express my sincere thanks to my supervisor Dr. Lennart Vamling for his excellent supervision and encouragement during the course of this research work.

Further I wish to express my thanks to Professor Thore Berntsson, to my fellow graduate students and staff members at the department of Heat and Power Technology for all their help in many respects.

I am also thankful to Britt-Marie Wanhov for retyping this manuscript, Bengt Erichsen for drawing figures and Cecilia Gabriellii for sharing her knowledge of condensation of mixtures.

Special thanks are due to Mr. Jon van Leuven, for proof-reading the manuscript.

I wish to thank Sabroe Refrigeration AB for collaboration and providing the experimental data, the Swedish National Board for Industrial and Technical Development (NUTEK), and the Swedish National Energy Administration, for financial support.

7. References

1. G. Ackermann, "Forschungsheft", 1934, No. 382, pp. 1-16.
2. Beatty, K.O., and Katz, D.L., "Condensation of vapours on outside of finned tubes", Chem. Eng. Prog., 1948, Vol. 44, pp. 55-70.
3. Blanc, Ph., Bontemps, A., Marvillet, Ch., "Condensation Heat Transfer of HCFC22 and HFC134a Outside a Bundle of Horizontal Low Finned Tubes", Proc. Int. Conf., CFCs, The Day After Padova, 1994, pp. 635-642
4. Briggs, A., Wen, X.L., Rose, J.W., "Accurate Heat Transfer Measurement for Condensation on Horizontal, Integral-Fin Tubes", Journal of Heat Transfer, 1992, Vol. 114, pp. 719-726.
5. Briggs, A., Rose, J.W., "Condensation Performance of Some Commercial Integral Fin Tubes With Steam and CFC113", Experimental Heat Transfer, 1995, Vol. 8, pp. 131-143.
6. Briggs, A., Rose, J.W., "Effect of fin efficiency on a model of condensation heat transfer on a horizontal, integral-fin tube", Int. J. Heat Mass Transfer, 1994, Vol. 37, Suppl.1, pp. 457-463.
7. Butterworth, D., "Inundation Without Vapour Shear", in Power Condensers and Heat Transfer Technology, 1981, Eds. Marto, P.J. and Nunn, R.H., pp. 271-278.
8. Cavallini, A., Col D. Del, Doretto, L., Longo G.A., Rossetto, L.M, "Experimental and Theoretical Investigation on Condensation Inside and Outside Enhanced Tubes", 36th European Two-Phase Flow Group Meeting at Portoroz, Slovenia, June 1-5, 1998.
9. Cavallini, A., Doretto, L., Longo, G.A., Rossetto, L; "A New Model for Forced Convection Condensation on Integral-Fin Tubes", Journal of Heat Transfer, 1996, Vol. 118, pp. 689-693.
10. Chilton, T.H., Colburn, A.P., "Mass Transfer (Absorption) Coefficients, Prediction from Data on Heat Transfer and Fluid Friction", Industrial and Engineering Chemistry, 1934, Vol. 16, No. 11, pp. 1183-1187.
11. Colburn, A.P., Drew, T.B., "The Condensation of Mixed Vapours", AIChE, 1937, Vol. 33, pp. 197-214.
12. Colburn, A.P., Wilmington, Del., Hougen, O.A., "Design of Cooler Condensers for Mixtures of Vapours with Noncondensing Gases", Industrial and Engineering Chemistry, 1934, Vol. 26, pp 1178-1182.

13. Fuller, E.N., Schettler, P.D., Giddings, J.C., "A New Method For Prediction Of Binary Gas-Phase Diffusion Coefficients", *Industrial and Engineering Chemistry*, 1966, Vol. 58, No. 5, pp. 19-27.
14. Gabriellii, C., Vamling, L., "Replacement of R22 in shell-and-tube condensers: Experiments and simulations", *International Journal of Refrigeration*, 1997, Vol. 20, pp. 165-178.
15. Gogonin, I.I., Kabov, O.A., "An Experimental Study of R-11 and R-12 Film Condensation on Horizontal Integral-Fin Tubes", *Journal of Enhanced Heat Transfer*, 1996, Vol. 3, pp. 43-53.
16. Grant, I.D.R., Osment, B.D.J., "The Effect of Condensate Drainage on Condenser Performance", 1968, NEL Report No. 350.
17. Hijikata, K., et al., "Forced convective condensation of binary mixture of vapours", *JSME Int. Journal*, 1987, Vol. 30(270), pp. 1951-1956.
18. Hijikata, K., et al., " Forced convective condensation of binary mixture of vapours (2nd report). Condensation on vertical and horizontal tubes", *Trans. JSME (B) Int. Journal*, 1989a, Vol. 55(10), pp. 3190-3198.
19. Hijikata, K., et al., " Forced convective condensation of a zeotropic binary mixture on vertical and horizontal tubes", *Proc. 9th Int. Heat Transfer Conf.*, Israel, 1990, Vol.3, pp. 271-276.
20. Hijikata, K., "Free convective filmwise condensation of a binary mixture of vapours", *Proc. 8th Int. Heat Transfer Conf.*, San Francisco, 1986, Vol.4, pp. 1621-1626.
21. Honda, H., Uchima, B., Nozu, S., Nakata, H., Torigoe, E., "Film Condensation of R-113 on Inline Bundles of Horizontal Finned Tubes", *Journal of Heat Transfer*, 1991, Vol. 113, pp. 479-486.
22. Honda, H., Nozu, S., "A Prediction Method for Heat Transfer During Film Condensation on Horizontal Low Integral-Fin Tubes", *ASME Journal of Heat Transfer*, 1987, Vol. 109, pp. 218-225.
23. Honda, H., Takamatsu, H., Takada, N., Makishi, O., "Condensation of HCFC123 in bundles of horizontal finned tubes: effects of fin geometry and tube arrangement", *Int. J. Refrig.*, 1996, Vol. 19, No. 1, pp. 1-9.
24. Honda, H., Nozu, S., "A Generalized Prediction Method For Heat Transfer During Film Condensation On A Horizontal Low Finned Tube", *Proc. 2nd ASME –JSME Thermal Engineering Joint Conference*, P.J. Marto and I. Tanasawa, eds., 1987, *JSME Vol.4*, pp. 385-392.
25. Honda, H., Nozu, S., Takeda, Y., "A Theoretical Model of Film Condensation in a Bundle of Horizontal Low Finned Tubes", *Journal of Heat Transfer*, 1989, Vol. 111, pp. 525-532.
26. Katz, D.L., Geist, J.M., "Condensation on Six Finned Tubes in a Vertical Row", *Trans. ASME*, 1948, Vol. 70, pp. 907-914.
27. Kern, D.Q., "Mathematical Development of Loading in Horizontal Condensers", *AIChE Journal*, 1958, Vol. 4, pp. 157-160.

28. Krishna, R., Standart, G.L., "A Multicomponent Film Model Incorporating a General Matrix Method of Solution to the Maxwell-Stefan Equations", *AIChE Journal*, 1976, Vol. 2, No. 2, pp. 383-389.
29. Marto, P.J., "An Evaluation of Film Condensation on Horizontal Integral-Fin Tubes", *Journal of Heat Transfer*, 1988, Vol. 110, pp. 1287-1305.
30. Marto, P.J., "Film Condensation Heat Transfer Measurements On Horizontal Tubes: Problem and Progress", *Experimental Thermal and Fluid Sciences*, 1992, pp. 556-569.
31. Murphy, R.W. et al., "Condensing heat transfer for R114/R12 mixture on horizontal finned tubes", *Int. J. Refrig.*, 1988, Vol.11, pp. 361-366.
32. Nozu, S., et al., "Condensation of the zeotropic refrigerant mixture R114/ R113 in a horizontal annulus with an enhanced inner tube (experimental results)", *Trans. JSME(B)*, 1991a, Vol. 5783, pp. 645-652.
33. Nusselt, W., "Die Oberflächen-Kondensation des Wasserdampfes", 1916, *VDI Zeitung*, Vol. 60, 541-546, 569-575.
34. Rose, J.W., "Condensation on low finned tubes: An equation for vapour-side enhancement", *Condensation and Condenser Design ASME* 1993, pp. 317-327.
35. Smith, R.A., "VAPOURISER Selection, Design & Operation", Longman Scientific & Technical UK England, 1986, pp. 98-106.
36. Tamir, A. Merchuk, J.C., "Verification of a theoretical model for multicomponent condensation", *Chem. Engr. Journal*, 1979, Vol. 17, pp. 125-139.
37. Toor, H.L., "Diffusion in Three-component Gas Mixtures", 1957, *ibid.*, 3, 198.
38. Webb, R.L., Rudy, T.M., Kedzierski, M.A., "Prediction of The Condensation Coefficient on Horizontal Integral-Fin Tubes", *Journal of Heat Transfer*, 1985, Vol. 107, pp. 369-376.
39. Stewart, W.E., Prober, R., "Matrix Calculation of Multicomponent Mass Transfer in Isothermal Systems", *Ind. Eng. Chem. Fundamentals*, 1964, Vol. 3, pp. 324.
40. Stephan, K. "Heat transfer in condensation and boiling", Springer Verlag, Berlin, 1992.

